

# Nuclear like effects in proton-proton collisions at high energy

L. Cunqueiro<sup>1</sup>, J. Dias de Deus<sup>2</sup> and C. Pajares<sup>1</sup>

<sup>1</sup>Departamento de Física de Partículas, Universidade de Santiago de Compostela  
and Instituto Galego de Física de Altas Enerxías (IGFAE),  
E-15782 Santiago de Compostela, Spain.

<sup>2</sup>CENTRA, Instituto Superior Técnico, 1049-001 Lisboa, Portugal.

## ABSTRACT

We show that several effects considered nuclear effects are not nuclear in the sense that they do not only occur in nucleus-nucleus and hadron-nucleus collisions but, as well, they are present in hadron-hadron (proton-proton) collisions. The matter creation mechanism in  $hh$ ,  $hA$  and  $AA$  collision is always the same. The  $p_T$  suppression of particles produced in large multiplicity events compared to low multiplicity events, the elliptic flow and the Cronin effect are predicted to occur in  $pp$  collisions at LHC energies as a consequence of the obtained high density partonic medium.

The “nuclear effects” considered in high energy strong interacting physics are essentially not nuclear but resulting from the partonic medium dictated by the underlying theory, QCD. The physics in central  $pp$  collisions is not physics in vacuum but physics in a medium whose properties are universal. At very high energy the wave function of the initial protons contains a high number of partons in such a way that the partons of each proton probe a high density medium. As we shall see, the “nuclear modification factor”  $R_{AB}$  [1] or the distribution ratio central/peripheral,  $R_{CP}$ [1], and the “elliptic flow” parameter  $v_2$  [2][3], for instance, can be applied to  $pp$  collisions.

Note that to understand  $hA$  and  $AA$  collisions we need theoretical high energy nuclear physics, namely Glauber calculus [4]. Without it we could not estimate cross-sections, rescattering effects, the number of binary collisions or the number of participating nucleons. Of course, in  $pp$  collisions  $N_{coll} = 1$ ,  $N_{part} = 1$ .

We formulate our arguments in the frame of the string percolation model [5], but we think that the same formulation is valid in the Color Glass Condensate model [6]. Both of them are able to reproduce most of the RHIC data, obtaining a similar transverse momentum scale [7][8]; the saturation momentum scale  $Q_s$  and the percolation threshold are related to each other [9]. The discussed effects are a consequence of the high density partonic medium formed in the collision, independently of the detailed framework used for the description.

The similarities of  $hh$  and  $AA$  collisions were previously explored two decades ago [10][11] studying a hydrodynamical description of  $AA$  and  $\bar{p}p$  fluctuations and the dependence of the mean transverse momentum on the multiplicity.

In the string percolation model, multiparticle production is described in terms of color strings stretched between the partons of the projectile and the target. These strings decay into new ones by  $q\bar{q}$  or  $qq - \bar{q}\bar{q}$  pair production and subsequently hadronize to produce the observed hadrons. Due to confinement, the color of these strings is confined to a small area in transverse space  $S_1 = \pi r_0^2$ , with  $r_0 \simeq 0.2 - 0.3$  fm. With increasing energy and/or atomic number of the colliding particles, the number of strings  $N_s$  grows and they start to overlap forming clusters, very much like disks in two-dimensional percolation theory. At a certain critical density, a macroscopical cluster appears, which marks the percolation phase transition [12] [13]. This density corresponds to the value of  $\eta = N_s \frac{S_1}{S_A}$ ,  $\eta_c = 1.2$ , where  $S_A$  stands for the overlapping area of the colliding objects. A cluster of  $n$  strings behaves as a single string with energy-momentum corresponding to the sum of the individual ones and with a higher color field corresponding to the vectorial sum in color space of the color fields of the individual strings. In this way, the mean multiplicity  $\langle \mu_n \rangle$  and the mean transverse momentum squared  $\langle p_{T_n}^2 \rangle$  of the particles produced by a cluster are given by

$$\langle \mu_n \rangle = \sqrt{\frac{nS_n}{S_1}} \langle \mu_1 \rangle \quad \text{and} \quad \langle p_{T_n}^2 \rangle = \left( \frac{nS_1}{S_n} \right)^{1/2} \langle p_{T_1}^2 \rangle, \quad (1)$$

where  $\langle \mu_1 \rangle$  and  $\langle p_{T_1}^2 \rangle$  are the corresponding quantities in a single string.

In the limit of random distribution of strings, eqs. (1) transform into:

$$\langle \mu \rangle = N_S F(\eta) \langle \mu_1 \rangle \quad \langle p_T^2 \rangle = \frac{\langle p_{T_1}^2 \rangle}{F(\eta)} \quad (2)$$

with  $F(\eta) = \sqrt{\frac{1 - \exp - \eta}{\eta}}$ .

If we are interested in a specific kind of particle  $i$ , we will use  $\langle\mu_1\rangle_i$ ,  $\langle p_{T1}^2\rangle_i$ ,  $\langle\mu_n\rangle_i$  and  $\langle p_{Tn}^2\rangle_i$  for the corresponding quantities. The transverse momentum distributions can be written as a superposition of the transverse momentum distributions of each cluster,  $g(x, p_T)$ , weighted with the distribution of the different tension of the clusters, i.e the distribution of the size of the clusters,  $W(x)$  [8] [14]. For  $g(x, p_T)$  we assume the Schwinger shape,  $g(x, p_T) = \exp(-p_T^2 x)$  and for the weight function,  $W(x)$ , the Gamma distribution  $W(x) = \frac{\gamma}{\Gamma(k)} (\gamma x)^{k-1} \exp(-kx)$  with  $\gamma = k/\langle x \rangle$  and  $k = \langle x \rangle^2 / (\langle x^2 \rangle - \langle x \rangle^2)$ .  $x$  is proportional to the inverse of the tension of each cluster, precisely  $x = 1/\langle p_{Tn}^2 \rangle = \sqrt{\frac{S_n}{nS_1}} \frac{1}{\langle p_{T1}^2 \rangle}$ .  $k$  is proportional to the inverse of the width of the distribution on  $x$  and depends on  $\eta$ .

The transverse momentum distribution  $f(p_T, y)$  is:

$$\frac{dN}{dp_T^2 dy} = \int_0^\infty dx W(x) g(p_T, x) = \frac{dN}{dy} \frac{k-1}{k} \frac{1}{\langle p_{T1}^2 \rangle_i} F(\eta) \frac{1}{\left(1 + \frac{F(\eta) p_T^2}{k \langle p_{T1}^2 \rangle_i}\right)^k} \quad (3)$$

Eq. (3) is valid for all densities and types of collisions. It only depends on the parameters  $\langle p_{T1}^2 \rangle_i$ . At low density  $\eta$ , there is no overlap between strings and therefore there are no fluctuations on the cluster size; all the clusters have only one string and  $k$  goes to infinity. At very high density  $\eta$ , there is only one cluster formed by all the produced strings. Again there are no fluctuations,  $k$  tends to infinity and the transverse momentum distribution recovers the exponential shape. In between these two limits,  $k$  has a minimum for intermediate densities corresponding to the maximum of the cluster size fluctuations. The quantitative dependence of  $k$  on  $\eta$  was obtained from the comparison of equation (3) with RHIC  $AA$  data at different centralities. The peripheral  $Au$ - $Au$  collisions at RHIC correspond to  $\eta$  values slightly above the minimum of  $k$ . Notice, that according to eq. (3) the ratio  $R_{CP}$  is, at intermediate and high  $p_T$ , proportional to  $p_T^{2(k-k')}$ , being  $k$  and  $k'$  the corresponding values for peripheral and central collisions respectively. As  $k' > k$ ,  $R_{CP}$  is suppressed.

The equations (2) and (3) must be slightly modified in the case of baryons to take into account the differences between mesons and baryons in the fragmentation of a cluster of strings due to both the higher color and the higher possibilities of flavor recombination [14]. Due to this, eq. (2) becomes for (anti)baryons:

$$\mu_{\bar{B}} = N_S^{1+\alpha} F(\eta_{\bar{B}}) \mu_{1\bar{B}} \quad (4)$$

where  $\alpha \sim 0.09$  and  $\mu_{1\bar{B}} \sim 0.033 \mu_{1\pi}$ . This means that the density  $\eta$  must be replaced by  $\eta_{\bar{B}} = N_S^\alpha \eta$ .

In figs. 1 and 2 we show the ratio  $R_{CP}$  between the inclusive  $pp$  going to  $\pi$ ,  $k$  and  $\bar{p}$  cross sections for events with a multiplicity twice larger than the mean multiplicity and the minimum bias cross-sections at LHC and RHIC energies respectively. The values of the parameters used are  $\langle p_{T1}^2 \rangle_\pi = 0.06 \text{ GeV}^2/c$ ,  $\langle p_{T1}^2 \rangle_K = 0.14 \text{ GeV}^2/c$  and  $\langle p_{T1}^2 \rangle_{\bar{p}} = 0.3 \text{ GeV}^2/c$ . It is clear why the  $p_T$  dependence of  $R_{CP}$  changes so much when moving from RHIC to LHC. At RHIC we are still in the low string density regime, with  $k$  decreasing with  $\eta$ . Since  $R_{CP} \sim p_T^{2(k-k')}$ , and  $k > k'$ , there is no suppression. On the contrary, at LHC for high density events we are above the minimum of  $k$ ,  $k < k'$  and  $R_{CP}$  is suppressed.

The values of  $\eta$  are computed using for  $N_S$  the values obtained from the quark gluon string model of reference [15], whose values are similar to the ones obtained using the dual

parton model [16] or Venus [17]. Essentially, they are the number of collisions times the number of strings per collision. This last number is twice the number of pomerons in  $pp$  collisions at a given energy.

We do not claim to describe all the data including high  $p_T$ . It is well known that jet quenching is the mechanism responsible for the high  $p_T$  suppression. This phenomenon is not included in our formula, which was obtained assuming a single exponential for the decay of a cluster without a power-like tail. Our formula, must be considered as a way of interpolating and of joining smoothly the low and intermediate  $p_T$  region with the high  $p_T$  region. Indeed the high  $p_T$  suppression implies by continuity a suppression of the highest  $p_T$  values of the intermediate region which are described by our formula (3). Therefore we have confidence in our results for low and moderate  $p_T$ , what means that our evaluations are valid for  $p_T$  less than 2-3 GeV/c at RHIC energies and 4-5 GeV/c at LHC energies. Outside this range our evaluations cannot be applied.

The density of partonic matter is at the origin of the observed scaling law of the elliptic flow,  $v_2$ , normalized to eccentricity ( $\epsilon$ ), that depends only on the particle density, i.e, the ratio between  $dN_{ch}/dy$  and the overlapping area  $S$  [1], independently of the energy, type and degree of centrality of the collision. Assuming that this scaling stands also for  $pp$  collisions, we can deduce  $v_2$  from the observed experimental scaling and from the values of  $\epsilon$ ,  $dN_{ch}/dy$  and  $S$ . Given a degree of centrality, we compute the impact parameter  $b$  using the code of reference [15]. The overlapping area and the eccentricity depend on the impact parameter and on the nuclear radius  $R_A$ :  $S = 2R_A^2 \cos^{-1}(\frac{b}{2R_A}) - b\sqrt{R_A^2 - \frac{b^2}{4}}$  and  $\epsilon = (\sqrt{2R_A + b} - \sqrt{2R_A - b})/(\sqrt{2R_A + b})$ .  $\frac{dN_{ch}}{dy}$  is taken from an extrapolation of  $pp$  data to the LHC in [18].

In any interacting partonic framework, it is natural to assume that the scaling law can be extended from  $AA$  to  $pp$  collisions. In our case, in fact, the strings, which are stretched between projectile and target partons, interact to form clusters regardless of the initial state particles being protons or nuclei.

The experimental measurement of  $v_2$  requires high multiplicities but the values of  $v_2$  corresponding to central events in  $pp$  collisions are quite negligible. In table 1 we show the obtained values of  $v_2$  for LHC and RHIC energies for  $pp$  minimum bias and also for central  $pp$  collisions at LHC energies assuming the mentioned empirical scaling. We see, that at LHC for minimum bias the elliptic flow  $v_2$  is comparable to the corresponding one for  $Au-Au$  collisions at  $N_{part} \simeq 250$  [19]. However, the charge multiplicity is not high enough ( $N_{ch} \simeq 80$ ) [20] what makes the measurement of  $v_2$  hard. Needless to say that a higher  $v_2$  can be obtained for more  $pp$  peripheral collisions, but in this case the charged multiplicity is lower being the measurement not feasible.

A more detailed evaluation of  $v_2$  done recently [21] in the framework of percolation of strings agrees with the values of table 1.

On the other hand, one can ask for the possibility of disappearance of back to back jet-like hadron correlations in  $pp$  as in the case of  $Au-Au$  collisions. Let us assume a hard quark-quark collision produced in the surface of a proton-proton collision. One outgoing quark will originate the trigger jet and the other back quark has to go through the strings stretched between the projectile and the target partons. The momentum broadening due to

	$\sqrt{s}$	$b$ (fm)	$\epsilon$	$S$ (fm <sup>2</sup> )	$dN_{ch}/dy$	$v_2$
$pp$ 0 – 10%	14 TeV	0.36	0.17	2.42	12-15	0.008
$pp$ min bias	14 TeV	1.18	0.49	0.93	6	0.035
$pp$ min bias	0.2 TeV	0.8	0.35	1.58	3	0.004

Table 1:  $v_2$  in  $pp$  collisions for different centralities together with the corresponding values for the energy, impact parameter, eccentricity, overlapping area and charged central rapidity distribution.

the interaction of the quark with one string has been computed in [8] to be

$$\Delta p_1 = \frac{4\pi\alpha_S}{3\sqrt{2}r_0} \simeq 0.9 - 0.75 \text{ GeV}/c$$

which is taken from the momentum of the quark. The average number of strings crossed by the quark is  $N = 2L \frac{r_0}{\pi R_p^2} N_S$  where  $L$  is the distance traveled by the quark  $L \simeq R_p$ . For very central  $pp$  collisions (multiplicity three times larger than the minimum bias multiplicity)  $N_S \simeq 40$  and for  $r_0 \simeq 0.2 - 0.3$  fm we have  $N \simeq 5 - 8$ . As explained in [8], the total broadening behaves like  $N^{1/2}$ , therefore

$$\Delta p_{TOT} = \sqrt{N} \Delta p_1 \simeq 1.6 - 2.6 \text{ GeV}/c.$$

Therefore the loss is not large, although it would be appreciable for inclusive particle measurements in the range of  $p_T \simeq 5 - 10$  GeV/c.

Recently it has been shown that large long range rapidity correlations are expected to occur in pp at LHC as well as the ridge structure seen at RHIC [22].

Summarizing, in  $pp$  collisions at LHC energies, some nuclear like effects such as high  $p_T$  suppression, elliptic flow and long range rapidity correlations could occur. Also, some suppression of the back to back jet like hadron correlations could be detected. All these effects are consequences of the high density partonic medium.

## Acknowledgments

We thank N.Armesto and C. A. Salgado for discussions. LC and CP have been supported by MEC of Spain under project FPA2005-01963, by Xunta de Galicia (Consellería de Educación) and by the Spanish Consolider-Ingenio 2010 Programme CPAN (CSD2007-00042). LC has also been supported by MEC of Spain under a grant of the FPU Program.

## References

- [1] K. Adcox *et al.* [PHENIX Collaboration], Nucl. Phys. A **757**, 184 (2005); B. B. Back *et al.* [PHOBOS Collaboration], Nucl. Phys. A **757**, 28 (2005); I. Arsene *et al.* [BRAHMS Collaboration], Nucl. Phys. A **757**, 1 (2005); J. Adams *et al.* [STAR Collaboration], Nucl. Phys. A **757**, 102 (2005).

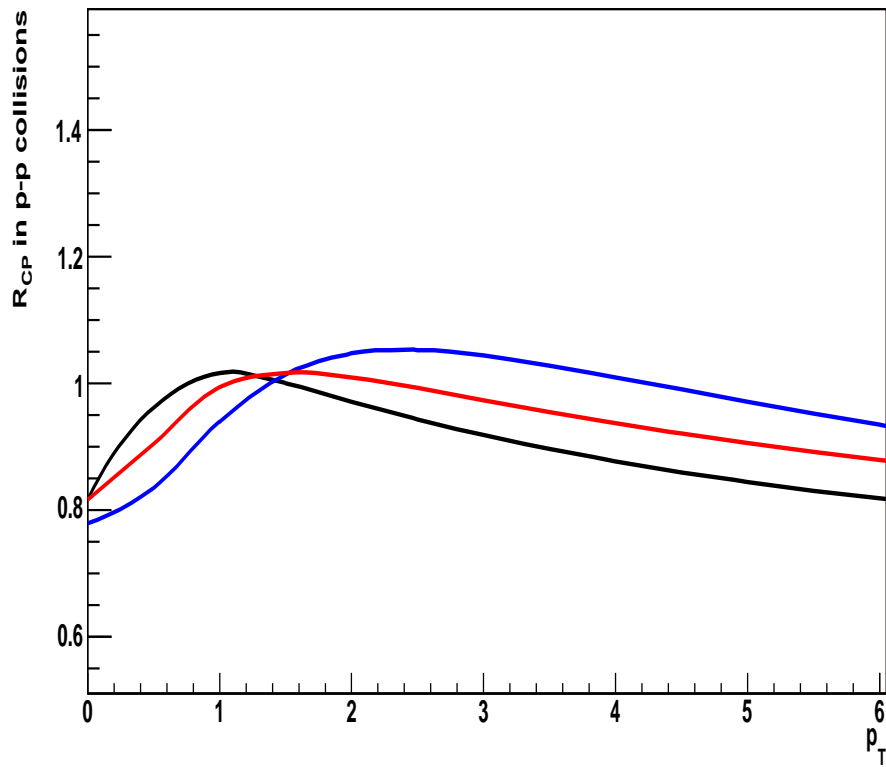


Figure 1: Central to peripheral ratio  $R_{CP}$  for pions (black), kaons (red) and antiprotons (blue) in  $pp$  collisions at LHC energies.

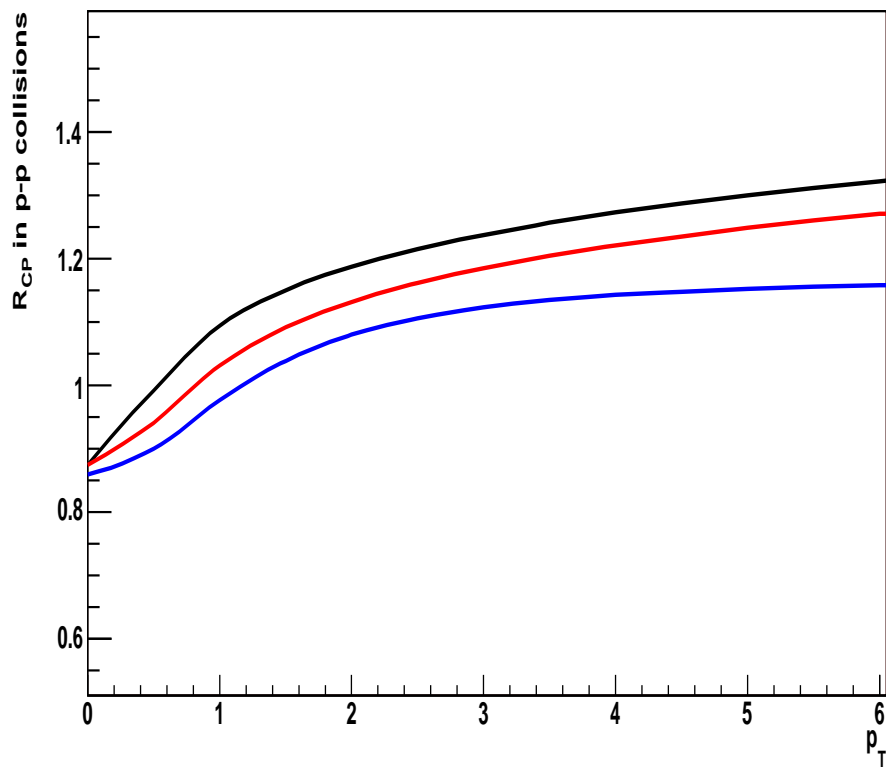


Figure 2: Central to peripheral ratio  $R_{CP}$  for pions (black), kaons (red) and antiprotons (blue) in  $pp$  collisions at RHIC energies.

- [2] S. S. Adler *et al.* [PHENIX Collaboration], Phys. Rev. Lett. **91** (2003) 182301.
- [3] C. Adler *et al.* [STAR Collaboration], Phys. Rev. Lett. **87** (2001) 182301.
- [4] R. J. Glauber and G. Matthiae, Nucl. Phys. B **21** (1970) 135.
- [5] N. Armesto, M. A. Braun, E. G. Ferreira and C. Pajares, Phys. Rev. Lett. **77** (1996) 3736; M. Nardi and H. Satz, Phys. Lett. B **442** (1998) 14.
- [6] L. D. McLerran and R. Venugopalan, Phys. Rev. D **49** (1994) 2233.
- [7] J. Schaffner-Bielich, D. Kharzeev, L. D. McLerran and R. Venugopalan, Nucl. Phys. A **705** (2002) 494.
- [8] J. Dias de Deus, E. G. Ferreira, C. Pajares and R. Ugoccioni, Eur. Phys. J. C **40** (2005) 229.
- [9] J. Dias de Deus and C. Pajares, Phys. Lett. B **642** (2006) 455.
- [10] H.von Gersdorff, L.D.McLerran, M. Kataja, P.V.Ruuskanen, Phys. Rev. D **34** (1986) 794.
- [11] L.D.McLerran, M. Kataja, P.V.Ruuskanen, H. von Gersdorff, Phys. Rev. D **34** (1986) 2755.
- [12] C. Pajares and Yu. M. Shabelski, “Relativistic Nuclear Interactions”, URSS, Moscow (2007).
- [13] C. Pajares, Eur. Phys. J. C **43** (2005) 9; J. Dias de Deus and R. Ugoccioni, Eur. Phys. J. C **43** (2005) 249.
- [14] L. Cunqueiro, J. Dias de Deus, E. G. Ferreira and C. Pajares, Eur. Phys. J. C **53** (2008) 585.
- [15] N. S. Amelin, N. Armesto, C. Pajares and D. Sousa, Eur. Phys. J. C **22** (2001) 149.
- [16] A. Capella, U. Sukhatme, C. I. Tan and J. Tran Thanh Van, Phys. Rept. **236** (1994) 225. A. Capella, C. Pajares and A. V. Ramallo, Nucl. Phys. B **241** (1984) 75.
- [17] K. Werner, Phys. Rept. **232** (1993) 87.
- [18] W. Busza in N. Armesto *et al.*, J. Phys. G **35** (2008) 054001.
- [19] B. B. Back *et al.* [PHOBOS Collaboration], Phys. Rev. Lett. **93** (2004) 082301.
- [20] S. G. Matinyan and W. D. Walker, Phys. Rev. D **59** (1999) 034022.
- [21] I. Bautista, L. Cunqueiro, J. Dias de Deus and C. Pajares, arXiv:0905.3058 [hep-ph].
- [22] P. Brogueira, J. Dias de Deus and C. Pajares, Phys. Lett. B **675** (2009) 308.